Article ID: 1007-7294(2014)09-1044-11

An Improved Moving Particle Semi-implicit Method for Dam Break Simulation

WU Qiao-rui[1], *TAN Ming-yi*[2], *XING Jing-tang*[2]

(1. Vibration and Shock Lab, Harbin Engineering University 150001, China; 2. FSI Group, Faculty of Engineering and the Environment, University of Southampton, SO17 1BJ, UK)

Abstract: Dam break is quite a common and hazard phenomenon in shipbuilding and ocean engineering. The objective of this study is to investigate dam break hydrodynamics with improved Moving Particle Semi-implicit method (MPS). Compared to traditional mesh methods, MPS is feasible to simulate surface flows with large deformation, however, during the simulation, the pressure oscillates violently, due to misjudgment of surface particles as well as particles gathering together. To modify these problems, a new arc method is applied to judge free surface particles, and a collision model is introduced to avoid particles from gathering together. Hydrostatic pressure is simulated by original and improved MPS. The results verify that improved MPS method is more effective. Based on these, dam break model is investigated with improved MPS.

Key words: particle method; semi-implicit; dam break

CLC number: U66 O39 **Document code**: A **doi:** 10.3969/j.issn.1007-7294.2014.09.004

1 Introduction

Dam break flood resulting from a sudden release of water due to the catastrophic collapse of dam (Fig.1) is a serious emviromental hazard, which causes loss of lives and huge enconomic damage[1]. For exmaple, the dam break accident in Xiangfen in 2008, as shown in Fig.2, casued about 300 death and the direct economic losses of 16 million dollars. Dam break flow becomes more challenging when it propagates over some obstacles, which plays an important role on the flow regime behavior at down stream. As a result, strong hydraulic jumps and discontinityor large deformation can occur. Hence, it is of great significance to minimize the catastrophic effects of the flood waves by forecasting the hazards. Both experimental[2-4] and numerical[5-7] methods are applied to investigate dam break problems. Among these numerical methods, meshless methods show great advantages in capturing free surface effeciently.

In recent years, meshless methods[8-9] have drew more and more attention in shipbuilding

Received date: 2014-04-18

Foundation item: Supported by the Fundamental Research Funds (No. HEUCF140115) and the Research Funds for State Key Laboratory of Ocean Engineering in Shanghai Jiao Tong University (No. 1310)

Biography: WU Qiao-rui(1986-), female, Ph.D. student in Ship Archetecture and Occean Engineering, Email: qiaoruidhd@163.com; TAN Ming-yi(1956-), male, lecturer/tutor of University of Southampton, E-mail: M.Tan@soton.ac.uk; XING Jing-tang (1951-), male, professor/tutor of University of Southampton, E-mail: jtxing@soton.ac.uk.

and ocean Engineering. Messless methods substitute meshes with particles to discretise the research object. Compared to traditional mesh methods, the difficulties of generating mesh and dealing with mesh mutation or drift can be avoided subtly, so mesh methods have absolute advantages in solving problems with large deformation. There are a variety of particle methods[10]. Among these methods, SPH and MPS are widely accepted and applied in many areas.

MPS is first proposed by Koshizuka and Oka[11] in 1996. MPS solves the Navier-stokes equation in a complete Lagrange way so that the numerical diffusion resulted from solving the convection term can be avoided. MPS becomes the hotspot of computational fluid dynamics in shipbuilding and ocean engineering. It has been applied successfully to simulate multi-phase flows[12-13], bubble dynamics[14], free surface flows[15] and fluid-structure interaction[16] problems. However, the oscillation of pressure is a barrier to the complete application of MPS in engineering. In this study, arc method and a collision model were employed to improve original MPS. And it was verified by hydrostatic pressure simulation. Based on these, different dam break models are investiged and analysed.

Fig.1 The instant of dam break

Fig.2 Dam accident in Xiangfen (Xi'an, 1980)

2 Basis of MPS

Prediction-correction model is applied to solve the Navier-Stokes equation. The first step is called prediction step. In this step, intermediate velocities and coordinates are calculated explicitly by the information of last time step. The second step is called correction step. The intermediate velocities are modified by solving Poisson equation. And then all the information in next time step is achieved.

2.1 Governing equations

For impressible viscous flows, the continuity equation (Law of mass conservation) and Navier- Stokes equation (Law of momentum conservation) are given by:

$$\begin{cases} \dfrac{\mathrm{d}\rho}{\mathrm{d}t}=\dfrac{\partial\rho}{\partial t}+\nabla\cdot(\rho v)=0 \\ \dfrac{\mathrm{d}v}{\mathrm{d}t}=f-\dfrac{1}{\rho}\nabla p+\upsilon\nabla^{2}v \end{cases} \tag{1}$$

where ρ is fluid density, v is fluid velocity, f is the external force, p is pressure and υ is the

kinematic viscosity coefficient.

2.2 Prediction–correction model

In the first step, the intermediate velocity components v^* are calculated using viscous diffusion term and external forces term (as shown in Eq.2), which are explicitly calculated with the values of r^n and v^n. Then intermediate r^* can be calculated by Eq.3:

$$v^*=v^n+\Delta t^*\left(f^n+\upsilon\nabla^2 v^n\right) \tag{2}$$

$$r^*=r^n+\Delta t^* v^* \tag{3}$$

In the second stage, the intermediate particle number densities n^* are obtained by the temporal coordinates r^*. The pressure in $n+1$ time p^{n+1} is calculated implicitly by Poisson equation in the following form:

$$\nabla^2 p^{n+1}=-\frac{\rho}{(\Delta t)^2}\frac{n^*-n_0}{n_0} \tag{4}$$

where n_0 is the initial particle number density. Then v^{n+1} and r^{n+1} can be obtained by the following two equations respectively:

$$v^{n+1}=v^*-\frac{\Delta t}{\rho}\nabla p^{n+1} \tag{5}$$

$$r^{n+1}=r^n+\frac{1}{2}\Delta t^*\left(v^n+v^{n+1}\right) \tag{6}$$

3 Numerical model of original MPS

3.1 Interaction model of particles

The kernel function proposed by Koshizuka and Oka[11] in 1996 is employed, which is used most widely in MPS:

$$w(r)=\begin{cases}\dfrac{r_e}{r}-1 & (r<r_e)\\ 0 & (r>r_e)\end{cases} \tag{7}$$

where r is the distance between particle, r_e is the effective radius of particle, the value of which directly affects the number of neighboring particles.

The number density of particle can be obtained by:

$$\langle n\rangle_i=\sum_{i\neq j} w\left(\left|r_i-r_j\right|\right) \tag{8}$$

The Gradient model is described by:

$$\langle\nabla\phi\rangle_i=\frac{d}{n^0}\sum_{j\neq i}\left[\left(\phi_j-\hat{\phi}_i\right)\frac{(r_j-r_i)}{\left|r_j-r_i\right|^2}W\left(\left|r_j-r_i\right|\right)\right] \tag{9}$$

where d is the dimemion, $\hat{\phi}_i$ is the minimum value of the neighboring particles of particle i, $\hat{\phi}_i$

$=\min(\phi_j)$, which is effective to avoid instability resulting from minus pressure gradient.

The Laplacian model of ϕ at point i is expressed as

$$\langle \nabla^2 \phi \rangle_i = \frac{2d}{n^0 \lambda} \sum_{j \neq i}^{N} [(\phi_j - \phi_i) W(|r_j - r_i|)] \tag{10}$$

where λ can be calculated by the following equation:

$$\lambda = \frac{\int_V w(r) r^2 \mathrm{d}V}{\int_V w(r) \mathrm{d}V} \cong \frac{\sum_{j \neq i}^{N} [W(|r_j - r_i|)|r_j - r_i|^2]}{\sum_{j \neq i}^{N} W(|r_j - r_i|)} \tag{11}$$

The effective radius $r_e=2.1L_0$ (L_0 is the initial distance of particles) is applied for particle number density, Gradient model and Laplacian model.

3.2 Stepping time condition

Since pressure is calculated implicitly by solving Poisson equation, the size of time step must be contrained in order to ensure stable and accurate results. The following Courant-Frendrichs-Levy(C-FL)[17] must be satisfied:

$$\Delta t \leqslant 0.1 \frac{L_0}{v_{\max}} \tag{12}$$

where L_0 is the initial distance of particles, $v_{\max}$ is predicted maximun particle velocity during the simulation. The factor 0.1 is introduced to ensure the particle moves only a fraction of particle spacing at each time step.

At the same time, another constraint prosposed by Cummins and Rudman[17] should be taken into account:

$$\Delta t \leqslant 0.125 \frac{L_0^2}{\mu/\rho} \tag{13}$$

where μ is the dynamic viscosity coefficient. Combining these two constraints, the time step is determined by:

$$\Delta t \leqslant \min\left(0.1 \frac{L_0}{v_{\max}}, 0.125 \frac{L_0^2}{\mu/\rho}\right) \tag{14}$$

3.3 Boundary condition

For the free surface boundary condition, the kinetic and dynamic boundary conditions are imposed. In the vicinity of free surface, the particle number densities decrease because of including the empty air region, where no particles exist. Thus, the free surface particles can be judged by:

$$\langle n \rangle_i^* < \beta n^0 \tag{15}$$

where β is a parameter below 1.0 and $\beta=0.97$ is selected in the study.

On the other hand, the dynamic free surface condition is satisfied by taking the atmospheric pressure $p=p_{atm}=0$ for the free surface particles.

In order to avoid misjudging the fluid particles near the boundary as free surface particles, the solid boundary is dicretised into three layers of particles. Moreover, a repulsive force[19] is employed to prevent fluid particles from penetrating the solid boundary, which is calculated in the following equation:

$$f(r)=D\left[\left(\frac{r_0}{r}\right)^{P_1}-\left(\frac{r_0}{r}\right)^{P_2}\right]\frac{r}{r^2}\quad (r>r_0) \tag{16}$$

where r_0 is usually set as L_0, $D=5gH$, H is the height of water column, $P_1=4$, $P_2=2$.

4 Two improvements of MPS

4.1 Arc method

Tab.1 Arc method

Particle 3		Particle 7	
Neighboring particle	Covered arc (clockwise)	Neighboring particle	Covered arc (clockwise)
1	(0, 0.367Pi)	1	(0, 0.417Pi)
10	(0.228 Pi, 0.706Pi)	8	(0.367 Pi, 0.711Pi)
2	(0.617Pi, 0.861Pi)	5	(0.644 Pi, 0.989Pi)
		4	(0.906 Pi, 1.311Pi)
		6	(1.278 Pi, 1.678Pi)
		9	(1.561 Pi, 1.844Pi)
		10	(1.756 Pi, 2.11Pi)
Overall covered arc: (0, 0.861Pi)		Overall covered arc: (0, 2.11Pi)	
Conclusion: Particle 3 is a free surface particle		Conclusion: Particle 7 is an inner particle	

As shown in Fig.4(a), the misjudgment of free surface particles happens sometimes, which will affect the calculation of pressure directly. Koh, Gao and Luo[20] used a new method called arc method, which is illustrated in Fig.3 and Tab.1. The principle of arc method is to check whether the particle is completely surrounded by its neighbouring particles. In other words, if the overal covered arc is beyond (0, 2Pi) without intervals, the particle is judged as inner fluid particle; other conditions are all judged as free surface particles.

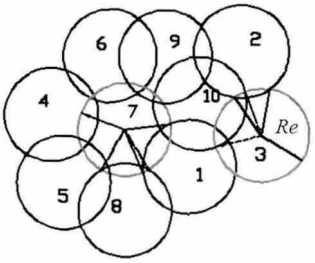

Fig.3 Illustration of Arc method

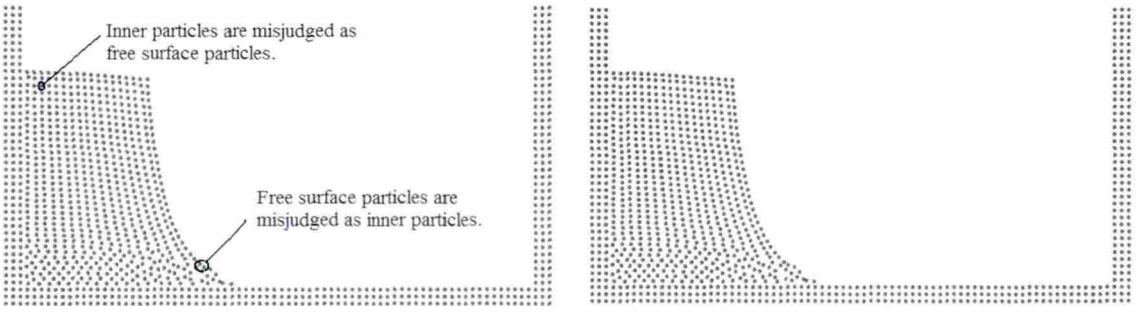

(a) Particle number density method (b) Arc method

Fig.4 Comparison of two judging methods

It can be seen from Fig.4 that compared to the particle number density method, arc method is more effective to identify free surface particles.

4.2 Collision model

In order to prevent particles from gathering, a collision model is introduced into MPS.

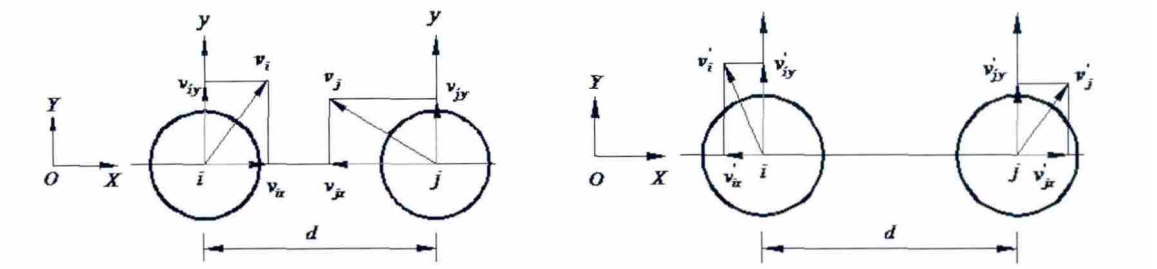

(a) Before collision　　(b) After collision

Fig.5 Collision model

As shown in Fig.5, OXY is overall coordinate system, and the coordinate with origin in the center of the particle is local coordinate system. When the distance of two particles satisfies $d<\beta L_0$, then the collision model is applied as:

$$mv_{ix}+mv_{jx}=mv_{ix}'+mv_{jx}' \tag{17}$$

where m is the particle mass, $v_{ix}'=-\alpha v_{ix}$. The optimal combination is α=0.2, β=0.99.

5 Numerical verification

The hydrostatic model is selected as shown in Fig.6(a). The simulation results are shown in Fig.6(b). It can be seen that the pressure calculated by original MPS fluctuates largely around the theoretical value, and it takes about 2 seconds for the pressure to stay close to the theoretical value, while the pressure obtained by improved MPS reaches the theoretical value in a very short time. Hence, the pressure occillation can be lessened to great extent by improved MPS.

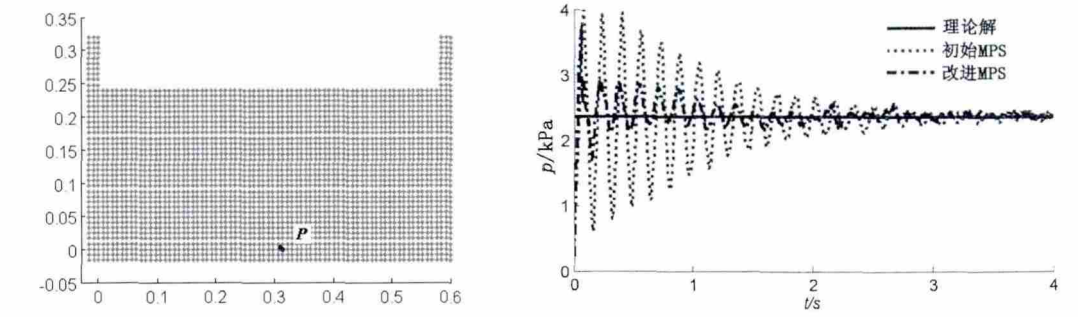

(a) Hydrostatic model　　(b) Compassion of pressure at P

Fig.6 Hydrostatic pressure simulation

6 Dam break simulation

6.1 Model of dam break without obstacle

The dam break model[21] is adopted here. As shown in Fig.7, the length and height of wa-

ter column and tanker are 1.2 m, 0.6 m and 3.22 m, 2 m, repectively. The initial distance between particles L_0 is 0.01 m, the time step is 0.000 5 s. The kinematic viscosity coefficient υ is set as 0.001. The pressure variation with time at P (3.22 m, 0.16 m) on the solid wall is detected and analysed during the simulation.

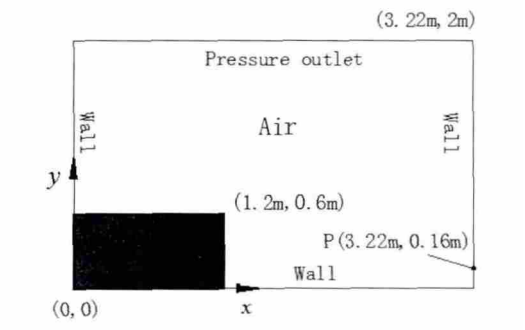

Fig.7 Model of dam break without obstacle

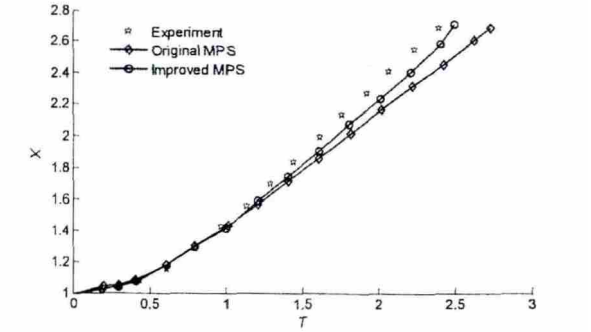

Fig.8 Comparison for position change of leadingedge of collapsed water column

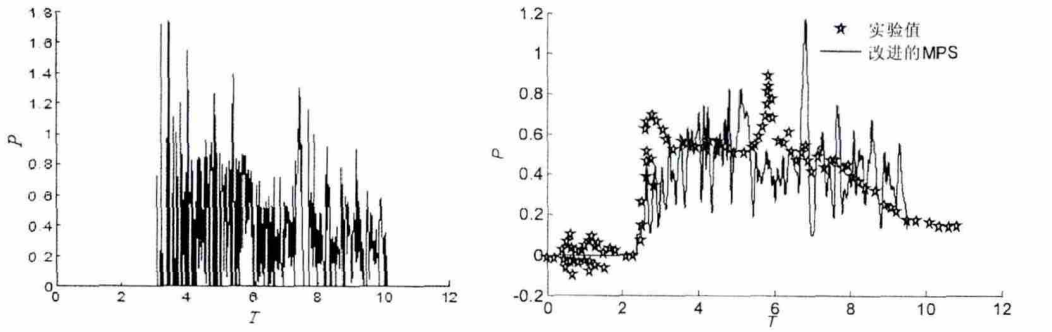

(a) Pressure change with original MPS (b) Pressure change with improved MPS

Fig.9 Comparison of pressure at point P

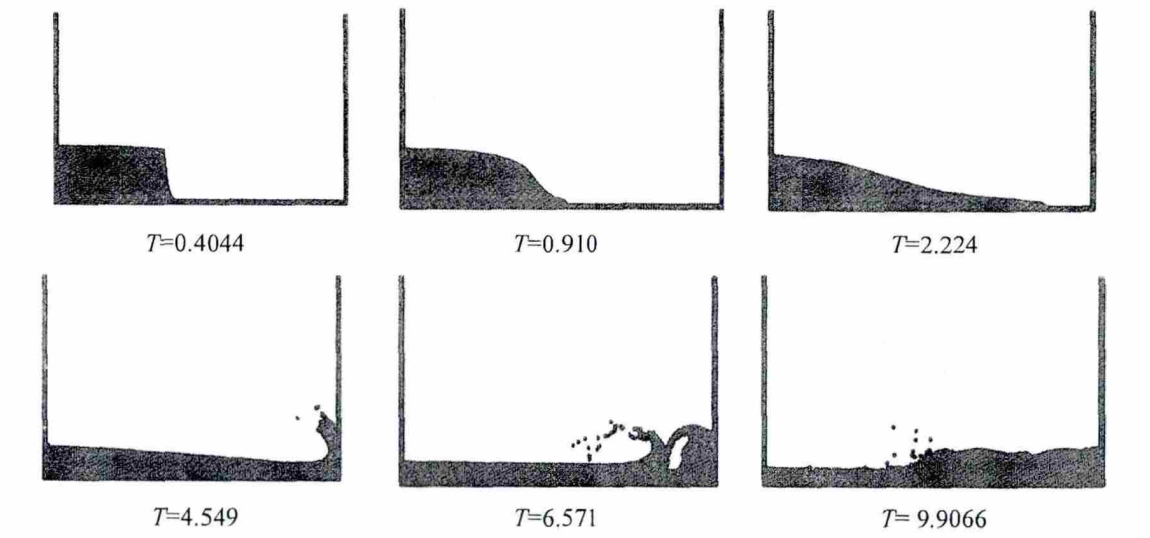

Fig.10 Dam break simulation

Fig.8 shows the position change of leading edge of collapsed water column, of which the horizontal and longitudinal ordinate are $X=x/L$ and $T=t\sqrt{2g/L}$, respectively. L is1.2 m, the

length of the water column. It can be seen from Fig.8 that the velocity of the leading edge is accelerated as soon as the dam break happens, then literally gets to a stable value. When $T\approx 2.5$, the leading edge arrives at the front solid wall. In Fig.9, the longitudinal ordinate is $P=p/\rho gh$. There are two pressure peaks during the process of dam break seen as in Fig.9. One happens at about $T\approx 3$, just after the leading edge arrives at the front, and the other occures at about $T\approx 6$, the reason of which can be deduced from the phenomenon of dam break shown in Fig.10 that the flow with high velocty shock at the wall, walks up along the wall, and then overturns, drops and hits the wall again. It also can be seen from Fig.9 that the second peak of pressure is much larger than the first one, which should be paid more attention in the prediction of hazards by dam break.

6.2 Model of dam break with obstacle

Next, the example of dam break with obstacle studied experimentally by Koshizuka et al[22] is investigaed, as shown in Fig.11. Here, L is 0.146 m and h is 0.024 m. The initial distance between particles L_0 is 0.01 m, the time step is 0.000 5 s. The kinematic viscosity coefficient υ is set as 0.001. The pressure at P1, P2, P3, P4 (the height is 0.016 m, 0.032 m, 0.048 m and 0.032 m) is invetigated.

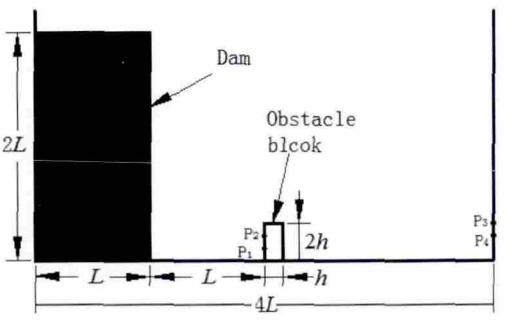

Fig.11　Model of dam break with obstacle

It can be seen from Fig.14 that the simulation results agree well with the experiment. Fig.11 shows the variation of pressure at P1 and P2. The pressure peaks happen when the collapsed water column arrives at the obstacle at about 0.17 s, then after that, the pressure literally decreases to the hydrostacic pressure; while in Fig.13, the pressure jumps due to the strong discontinity of water jet. Compared to P1and P2, the peak pressure at P3 and P4 is smaller, but the peak repeats many times.

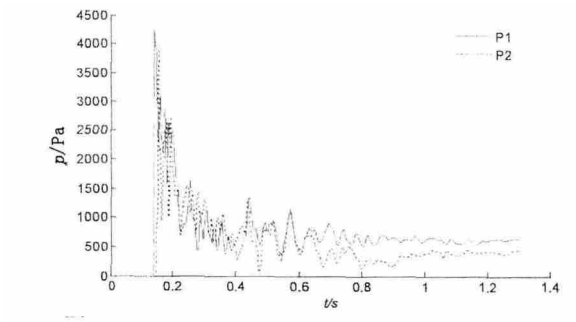

Fig.12　Pressure change with time at P1and P2

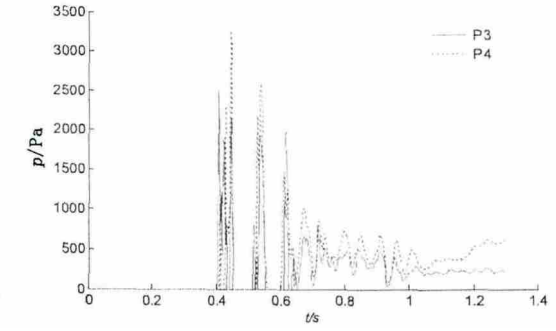

Fig.13　Pressure changing with time at P3and P4

t=0.1 s

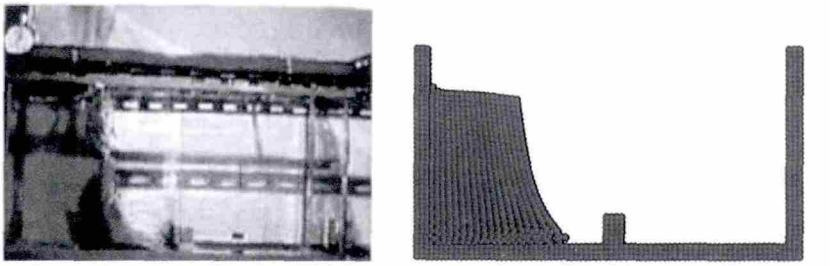

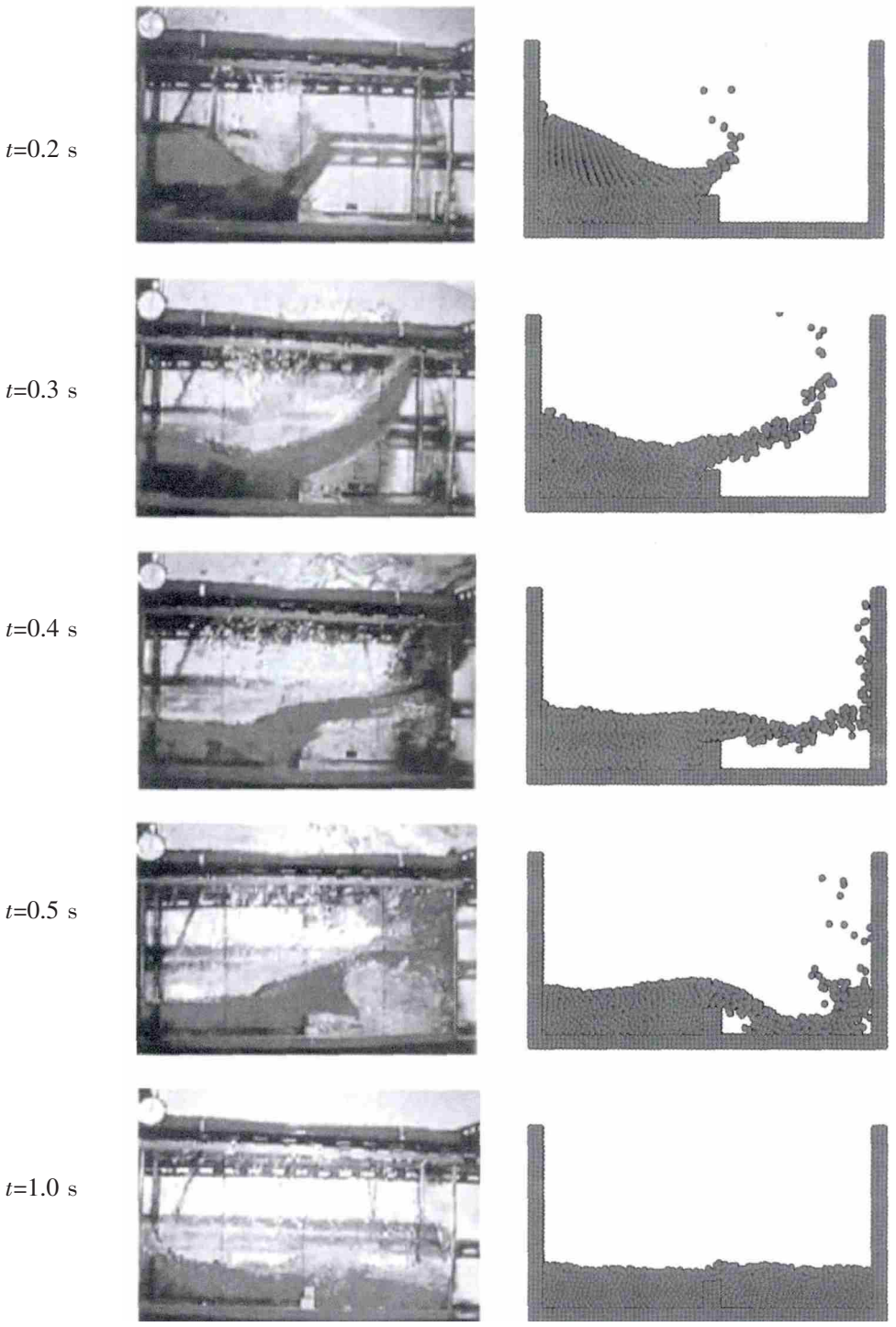

Fig.14 Dam break with obstacle: experimental results (photo) by Koshizuka et al[22] and numerical results

6 Conclusions

In the study, arc method and one collision model are introduced to the original MPS to improve the pressure oscillation. Hydrostatic pressure is simulated to verify improved MPS. Based on this, the models of dam break with and without obstacle are investigated, and the main con-

clusions are listed in the following:

(1) Arc method is quite an effective way to identify free surface particles. And collision model is feasible to avoid particles from gathering together The improved MPS with arc method and collision model is more compatible to simulate free surface flows.

(2) For the dam break without obstacle, there exists two pressure peak. One results from the direct shock of collapsed water column, and the other from overturning water shock. The second peak is larger so that it must be catiously checked when assessing the safety of the dam.

(3) For the dam break with obstacle, the front side of the obstacle affords a large shock force, which will be catactrophic to buildings suffered from a dam break nearby. Althogh pressure peak on the solid wall is smaller, however, the repetive force still can not be neglected.

Acknowledgements

This work is supported by the Fundamental Research Funds for the Central Universities (Grant No. HEUCF140115) and the Research Funds for State Key Laboratory of Ocean Engineering in Shanghai Jiao Tong University (Grant No. 1310).

References

[1] He X Y, Liang Z Y. The influence of dam break and overview of related risk estimate[J]. China Flood Control and Drought Relief, 2008, 6: 51–55.

[2] Martin J C, Moyce W J. Experimental study of the collapse of liquid columns on a rigid horizontal plan[J]. Philo- sophical Transactions of the Royal Society of London, 1952, 244: 312–324.

[3] Carrivich J L, Jones R and Keevil G. Experimental insights on geomorphological processes within dam break outburst floods [J]. Jounal of Hydrology, 2011, 408: 153–163.

[4] Xue Y, Xu W L, et al. Experimental study of dam-break flow in cascade reservoirs with steep bottom slope[J]. Journal of Hydrodamics, 2011, 23(4): 491–497.

[5] Park I R, Kim K S, Kim J and Van S H. Numerical investigation of the effects of turbulence intensity on dam-break flows [J]. Journal of Ocean Engineering, 2012, 42: 176–187.

[6] Chang T J, Kao H M, Chang K H and Hsu M H. Numerical simulation of shallow water dam break flows in open channels using smoothed particle hydrodynamics[J]. Journal of Hydrology, 2011, 408: 78–90.

[7] Jeong W, Yoon J S and Cho Y S. Numerical study on effects of building groups on dam-break flow in urban area[J]. Journal of Hydro-environment Research, 2012, 6: 91–99.

[8] Li S, Liu W K. Meshfree and particle methods and their applications[J]. Applied Mechanics Reviews, 2002, 55(1): 1–34.

[9] Belytschko T, Krongauz Y, Organ D, et al. Meshless methods: An overview and recent developments[J]. Computer Methods in Applied Mechanics and Engineering, 1996, 139: 3–47.

[10] Thomas P F, Matthies H G. Classification and overview of meshfree methods[J]. Germany Brunswich Informa-tikbericht, 2003.

[11] Koshizuka S, Oka Y. Moving-paricle semi-implicit method for fragmentation of incompressible fluid[J]. 1996, 123: 421–434.

[12] Sjalonaeomoa A, Jin Y C. MPS mesh-free particle method for multiphase flows[J]. Comput. Methods Appl. Mech. Engrg, 2012, 13: 229–232.

[13] Park S, Jeun G. Coupling of rigid body dynamics and moving particle semi-implicit method for simulation isothermal multi-phase fluid interactions[J]. Comput. Methods Appl. Mech. Engrg, 2011, 200: 130–140.

[14] Tian W X, Ishiwatari Y, et al. Numerical simulation on void bubble dynamics using moving particle semi-implicit method [J]. Nuclear Engineering and Design, 2009, 239: 2382–2390.

[15] Sun Z G, Liang Y Y and Xi G. Numerical simulation of the flow in straight blade agitator with MPS method[J]. Internatioal Journal for Numerical Methods in Fluids, 2011, 67: 1960–1972.

[16] Sueyoshi M, Kashiwagi M and Naito. J Mar Sci TechnolS. Numerical simulation of wave–induced nonlinear motions of a two–dimensional floating body bu the moving particle semi–implicit method[J]. J Mar Sci Technol, 2008, 13: 85–94.

[17] Shao S D, Lo Y M. Incompressible SPH method for simulating Newtonian and non–Newtonian flows with a free surface[J]. Advances in Water Resources, 2003, 26(7): 787–800.

[18] Cummins S, Murray R. An SPH projection method[J]. J Coumut. Phys, 1999, 152(2): 584–607.

[19] Monaghan J J. Simulation free surface flow with SPH[J]. Journal of Computational Physics, 1994, 110: 399–406.

[20] Koh C G, Gao M, Luo C. A new particle method for simulation of incompressible free surface flow problems[J]. International Journal for Numerical Methods in Engineering, 2012, 89: 1582–1604.

[21] Abdolmaleki K, Thiagarajan K P and Morris–Thomas M T. Simulation of the dam break problem and impact flows using a Navier–Stokes solver[C]// 15th Australian Fluid Mechanics Conference, December, 2004. The University of Sydney, Sydney, Australia, 2004: 13–17.

[22] Koshizuka S, Tamako H and Oka Y. A particle method for incompressible viscous flow with fluid fragmentation[J]. Computational Fluid Dynamics Journal, 1995, 4(1): 29–46.

基于改进的移动粒子半隐式方法的溃坝模拟

吴巧瑞[1], Tan Ming–yi[2], Xing Jing–tang[2]

(1 哈尔滨工程大学 振动冲击实验室, 哈尔滨 150001; 2 南安普顿大学环境工程系流固耦合组, 英国 南安普顿 SO17 1BJ)

摘要: 溃坝现象在船舶与海洋工程中是常见而又危险的,甲板上浪、液舱晃荡等都可以看作是广义的溃坝现象。溃坝是一种典型的自由面流动问题,存在运动边界以及复杂大变形和流体强间断问题,因此此类自由面流动的数值模拟一直是计算流体力学领域的一大难题。文章基于改进的移动粒子半隐式方法(MPS),对溃坝问题进行了研究分析。相对于传统的网格法,MP 在模拟大变形自由流动中展示了很大的优势。但是,在模拟过程中,由于自由表面粒子的误判以及粒子的过于集中现象,导致压力发生剧烈的震荡现象。针对这些问题,把角度判断法和一个碰撞模型引入传统的 MPS 进行改进。静水压力的模拟验证了改进后的 MPS 方法的有效性。在此基础上,文中对无障碍物溃坝和有障碍物溃坝模型进行了模拟和分析。

关键词: 粒子法; 半隐式; 溃坝

中图分类号: U66 O39 **文献标识码**: A

作者简介: 吴巧瑞(1986–),女,哈尔滨工程大学船舶与海洋工程系博士研究生,E–mail:qiaoruidhd@163.com;
Tan Ming–yi(1956–),男,南安普顿大学环境工程系讲师,博士生导师;
Xing Jing–tang(1951–),男,南安普顿大学环境工程系教授,博士生导师。